

1 **Phytoplankton blooms on the western shelf of Tasmania:**
2 **Evidence of a highly productive ecosystem**

3

4 **J. Kämpf¹**

5 [1]{School of the Environment, Flinders University, Adelaide, Australia}

6 Correspondence to: J. Kämpf (jochen.kaempf@flinders.edu.au)

7

8 **Abstract**

9 Satellite-derived chlorophyll-a data using the standard NASA-OC3 algorithm are strongly
10 biased by coloured dissolved organic matter and suspended sediment of river discharges,
11 which is a particular problem for the west Tasmanian shelf. This work reconstructs
12 phytoplankton blooms in the study region using a quadratic regression between OC3 data and
13 chlorophyll fluorescence based on the fluorescence line height data. This regression is derived
14 from satellite data of the nearby Bonney upwelling region, which is devoid of river
15 influences. To this end, analyses of 10 years of MODIS-aqua satellite data reveal the
16 existence of a highly productive ecosystem on the west Tasmanian shelf. The region normally
17 experiences two phytoplankton blooms per annum. The first bloom occurs during late austral
18 summer months as a consequence of upwelling-favourable coastal winds. Hence, the west
19 Tasmanian shelf forms a previously unknown upwelling centre of the regional upwelling
20 system, known as “Great South Australian Coastal Upwelling System”. The second
21 phytoplankton bloom is a classical spring bloom also developing in the adjacent Tasman Sea.
22 The author postulates that this region forms another important biological hot spot for the
23 regional marine ecosystem.

24

25

26

27

28

1 1 Introduction

2 Physical processes that enrich the euphotic zone with nutrients are principal agents of coastal
3 phytoplankton blooms. Such processes include upwelling, storm-induced mixing, internal
4 waves and river plumes. Despite elevated nutrient levels, high turbidity levels in river plumes
5 can suppress diatom growth (e.g., Chen *et al.*, 2003). Except for the situation of coastal
6 upwelling, vertical density stratification generally supports phytoplankton production, in
7 particular when the surface mixed layer is relatively shallow and coincides with the euphotic
8 zone. This situation supports the development of the spring bloom, which is characteristic of
9 temperate North Atlantic, sub-polar, and coastal waters (Mann and Lazier, 2006).

10 The southern shelves of Australia host a large seasonal coastal upwelling system (Kämpf *et*
11 *al.*, 2004; Kämpf, 2010). In response to south-easterly coastal winds, upwelling events occur
12 in austral summer months (December to April). This upwelling system, referred to as the
13 “Great South Australian Coastal Upwelling System”, consists of three upwelling centres
14 (**Figure 1**): the long-known Bonney upwelling (Rochford, 1977; Lewis, 1981; Schahinger,
15 1987; Griffin *et al.*, 1997) along the so-called Bonney coast, and an upwelling centre off the
16 southern tip of the Eyre Peninsula (Kämpf *et al.*, 2004). The latter region plays a vital role in
17 the life cycles of sardine (*Sardinops sagax*), anchovy (*Engraulis australis*), and southern
18 bluefin tuna (*Thunnus maccoyii*) (Ward *et al.*, 2006).

19 This study focusses on the west Tasmanian shelf. Throughout the year, the Zeehan Current
20 runs southeastward confined to the shelf break along the continental shelf edge of western
21 Bass Strait and western Tasmania (Cresswell, 2000). This current is the extension of the
22 South Australian Current, which itself is the continuation of the Leeuwin Current (Ridgeway
23 and Condie, 2004), but seasonally also entrains warm water formed during summer months
24 on the shelves of the western Great Australian Bight (Herzfeld, 1997). Currents within Bass
25 Strait are created by tides, winds, incident continental shelf waves and density-driven flows
26 (e.g., Sandery and Kämpf, 2005). Bass Strait is relatively shallow (~50-70 m) and main
27 pathway of currents is generally eastward (Sandery and Kämpf, 2007). Prominent
28 oceanographic features of Bass Strait are the existence of tidal mixing fronts on both sides of
29 the strait (Sandery and Kämpf, 2005), and the wintertime formation of a density-driven
30 overflow on the eastern side of the strait in vicinity of the Bass Canyon, known as the Bass
31 Strait Cascade (Tomczak, 1985). Based on sparse field data, Gibbs and co-workers (Gibbs *et*
32 *al.*, 1986) concluded that nutrient levels in Bass Strait are overall low (<1 μM in nitrate)

1 except for the eastern edge where nutrient concentrations reach high levels (up to 7 μM in
2 nitrate) in winter. According to these authors, chlorophyll-a levels in Bass Strait are also
3 generally low ($<0.5 \text{ mg/m}^3$) but show highest concentrations over the adjacent shelf, again in
4 winter. In austral winter, blue grenadier (*Macruronus novaezelandiae*) form spawning
5 aggregations on the west Tasmanian shelf, being a key food source for Australian fur seals
6 (*Arctocephalus pusillus doriferus*) (Hamer and Goldsworthy, 2006).

7 Earlier work (Connolly and Von der Borch, 1967) postulated that upwelling of cold sub-
8 Antarctic waters is the main reason for the occurrence of extensive temperate carbonates on
9 the southern Australian shelves. Isotopic studies (e.g., Wass *et al.*, 1970) validated this
10 upwelling model for the formation of cold water carbonates. Interestingly, modern cold-water
11 carbonate is also predominant sediment on the west Tasmanian shelf (Rao and Green, 1983).
12 Isotope-based findings of Rao and Adibi (1992) demonstrate upwelling seawater as the main
13 process responsible for the formation of carbonates in western Tasmania. Motivated by the
14 findings of Rao and Adibi (1992), this work explores phytoplankton blooms on the west
15 Tasmanian shelf and their underlying physical processes.

16

17 **2 Methodology**

18 This work is based on satellite data, coastal wind data, and time series of river discharges.
19 This work focusses on two time periods. The first period (1/1/1998 to 31/12/2000), also
20 studied by Kämpf *et al.* (2004), is adopted to establish initial evidence of the phytoplankton
21 dynamics on the west Tasmanian shelf. Data are extracted from the South East Fishery (SEF)
22 ocean movies (David Griffin, CSIRO, <http://www.marine.csiro.au/~griffin/SEF/>) based on the
23 SeaWiFS database (9 km spatial resolution). Chlorophyll-a data are calculated from the
24 standard OC3 algorithm, which can overestimate phytoplankton blooms in coastal waters in
25 the presence of coloured dissolved organic matter (CDOM or gelbstoff) and suspended
26 sediment (e.g., Shanmugam, 2011). Hereby it should be noted that of the 136 eight-day
27 segments of chlorophyll-a data, 35 segments (26%) are missing for the western Tasmanian
28 shelf due to cloud bias, mainly during austral winter/spring months. This first analysis
29 indicates that OC3-derived chlorophyll-a data are substantially modified by river discharges.

30 The second, extended study period (1/1/2005 to 31/3/2014) adopts MODIS-aqua satellite data
31 (4 km spatial resolution). Fluorescence Line Height (FLH) data are used to reconstruct

1 phytoplankton blooms (e.g., Xing *et al.*, 2007) for the west Tasmanian shelf. In the absence of
2 suitable field data, this reconstruction is based on a regression of FLH and OC3 data for the
3 nearby Bonney upwelling region, which is devoid of noticeable river influences. The
4 reconstructed time series of chlorophyll-a is then used in an event-based statistical analysis of
5 phytoplankton blooms in response to possible nutrient-supply events; that is, coastal
6 upwelling events and/or river plumes. To this end, all relevant data are converted to 8-day
7 segments in alignment with the satellite data, noting that SST data are not used in this event
8 analysis. For the west Tasmanian shelf, 90 (21%) of the total of 425 eight-day segments are
9 unusable due to cloud bias.

10 Wind data from the Cape Grim weather station (see Figure 1) are used to calculate the
11 classical upwelling index representative for the western Tasmanian shelf. This index is based
12 on the theoretical offshore volume transport in the surface Ekman layer and it is calculated
13 from:

$$14 \quad UI = \frac{|\tau|}{\rho_o |f|} \cos(\alpha - \alpha'), \quad (1)$$

15 where τ is wind stress, $\rho_o \approx 1026 \text{ kg/m}^3$ is seawater density, $f \approx -0.9 \times 10^{-4} \text{ s}^{-1}$ is the value of the
16 Coriolis parameter at 40°S , α is wind direction and α' is average coastline orientation, taken
17 equivalent to 160° (based on the meteorological convention that 0° refers to northerly winds).
18 Small variations of α' have little influence of the results (not shown). For initial comparison,
19 we also calculated the upwelling index for the Bonney upwelling system for the period from
20 1/1/1998 to 31/12/2000.

21 River discharge data for the western coast of Tasmania are sparse. Whilst there are no stream-
22 flow data for the Macquarie Harbour estuary, which is the largest freshwater source on the
23 western Tasmanian shelf, the only continuous time series of relevant river discharges that the
24 author could find is that of the Davey River, being located in the south of western Tasmania
25 (see Figure 1). Without further evidence, the author postulates that the Davey River outflow
26 can be taken as a proxy of that of other western Tasmanian rivers.

27

1 **3 Results and Discussion**

2 3.1 Initial evidence based on SeaWiFS data (1998-2000)

3 Coastal upwelling events on the southern shelves of Australia are associated with high-
4 pressure weather systems that create southeasterly coastal winds (Kämpf *et al.*, 2004). Due to
5 their spatial scale and the geometry of Australia's coastline, such weather patterns can also
6 initiate coastal upwelling on the western shelf of Tasmania. In early January 2000, for
7 example, a high-pressure weather system developed centred over the South Australian Basin
8 (**Figure 2**). This high-pressure system became blocked by a low pressure cell over Tasmania,
9 triggering coast-parallel, upwelling-favourable winds along both Australia's southern shelves
10 and the west coast of Tasmania. During this period, strong upwelling occurred in the
11 upwelling centres on the southern shelves (Kämpf *et al.*, 2004). During this event,
12 chlorophyll-a levels on the west Tasmanian shelf attained values of $\sim 3 \text{ mg/m}^3$ being of the
13 same order of magnitude as those observed in the upwelling centre along the Bonney coast
14 (**Figure 3a**). Upwelling-related negative SST anomalies can be identified in both regions
15 (**Figure 3b**). While the Bonney upwelling has pronounced temperature anomalies of 2-3°C,
16 temperature anomalies on the west Tasmanian shelf are relatively difficult to distinguish from
17 those in the ambient ocean which are of a similar range.

18 The time series of the upwelling indices for both regions (**Figure 4**) reveals that, similar to the
19 upwelling centres of Australia's southern shelves, coastal winds along the west coast of
20 Tasmania are, on average, upwelling favourable during austral summer months (December –
21 April). This indicates that both regions share similar wind-forced upwelling characteristics.
22 Earlier work by Kämpf *et al.* (2004) has overlooked this feature.

23 OC3 chlorophyll-a levels off the Bonney coast develop clear peaks during the austral summer
24 upwelling season, chlorophyll-a levels on the western shelf of Tasmania attain a complex
25 temporal structure (**Figure 5a**). In particular, large discrepancies in OC3 chlorophyll-a levels
26 between the regions occur in austral winter months, which is the period of enhanced river
27 discharges (**Figure 5c**).

28 The time series of SST (**Figure 5b**) reveals intermittent warming periods from May to July
29 (i.e., during late austral autumn and early winter). These warming events, which are more
30 pronounced along the Bonney coast than on the west Tasmanian shelf, are associated with
31 incursions of the South Australian Current (**Figure 6** shows an example). Being of shelf

1 origin, this current has low nutrient content (e.g., Herzfeld, 1997) and its appearance in the
2 study regions can be identified by decreases in OC3 chlorophyll-a levels in each year of the
3 time series (see Figure 5a).

4 The timing of some events of elevated OC3 chlorophyll-a levels on the west Tasmanian shelf
5 seem to coincide with the onset of spring blooms in the western Tasman Sea, where
6 chlorophyll-a levels seasonally peaked in October at a level of 0.8 mg/m^3 in the years 1998-
7 2000 (Tilburg *et al.*, 2002). It should be noted that the Bonney upwelling region is devoid of
8 such spring blooms.

9

10 3.2 Detailed Analysis based on MODIS-aqua data (2005-2014)

11 Given the absence of noticeable river influences, OC3 chlorophyll-a data for the Bonney
12 upwelling region can be taken as a proxy for phytoplankton levels. The time series for this
13 region confirms the pronounced annual periodicity of phytoplankton blooms (**Figure 7a**).
14 Average peak chlorophyll-a levels tend to slightly vary between the years, which reflects
15 interannual variations of the frequency and intensity of individual upwelling events in this
16 region. Middleton *et al.* (2007) speculated that the upwelling intensity is strongly modulated
17 by ENSO events, but the satellite data shown here are devoid of any dramatic interannual
18 variability that could be linked to ENSO variability.

19 In contrast to the Bonney upwelling, the OC3 data on the west Tasmanian shelf vary in a
20 highly irregular fashion and all year round (see Figure 7a), noting that both regions attain
21 peak values of up to 3 mg/m^3 . The upwelling index for the west Tasmanian shelf generally
22 attains positive values for austral summer months (**Figure 7b**). In some years, this index
23 indicates brief upwelling events outside the summer season. For instance, the year 2007 had
24 such an event in June, and other years (e.g. 2005 and 2013) had early upwelling-favourable
25 wind events in November, being mirrored by individual OC3 peaks (see Figure 7a). On the
26 other hand, the upwelling index also indicates events of strong downwelling-favourable
27 winds, such as in August 2009.

28 Overall, the discharge from the Davey River tends to peak in austral winter/spring with
29 markedly reduced flows during austral summer months (**Figure 7c**). An exception is the year
30 break of 2005/2006 which had a relatively strong riverine discharge occurring in
31 December/January.

1 For completeness, the author also included a time series of wind stress magnitude (**Figure**
2 **7d**), given that strong storms have the ability to modify phytoplankton blooms via changes in
3 the mixed-layer depth and potential entrainment of nutrient-rich water from below. On the
4 other hand, storms can also erode vertical structure of phytoplankton concentrations, thereby
5 removing the surface appearance of a phytoplankton bloom. For instance, the existence of
6 relatively strong winds (~2.5 Pa) in January 2007 might explain relatively low surface OC3
7 levels in west Tasmanian coastal water although winds were upwelling favourable. It should
8 be noted that periods of 3-7 days of relaxed winds after a brief upwelling event are deemed
9 optimal for phytoplankton accumulation (Wilkenson *et al.*, 2006). This relaxation effect is not
10 explored in the context of this work.

11 The NASA OC3 algorithm is unreliable for the west Tasmanian shelf due strong river
12 influences. While it gives reasonable results in rare occasions of coastal upwelling events in
13 the absence of river flows, it often misinterprets low productive river plumes as
14 phytoplankton blooms, which are absent in the FLH data (**Figure 8**). In order to reconstruct
15 chlorophyll-a levels for the west Tasmanian shelf, OC3 and FLH data can be related to each
16 other for the Bonney upwelling region (**Figure 9a**), where river influences are sparse. This
17 comparison indicates a quadratic regression of the form of:

$$18 \quad y = 0.25 + 0.3x^2, \quad (2)$$

19 where y is the reconstructed chlorophyll-a value, and x is the FLH value (derived from the
20 NASA Giovanni database) multiplied by 100. The associated RMS-error of 0.53 mg/m^3 is
21 acceptable, noting that discrepancies can be attributed to absorption properties of the
22 atmosphere and physiological variations in the phytoplankton (Xing *et al.*, 2007).
23 Nevertheless, the reconstructed chlorophyll-a time series (based on equation (2)) agrees well
24 with the original OC3 data (**Figure 10a**). As expected, there is a mismatch between OC3 and
25 FLH data on the west Australian shelf (**Figure 9b**) attributed to river discharges. In this
26 region, the reconstructed time series of chlorophyll-a differs substantially from that derived
27 from the OC3 algorithm (**Figure 10b**, compared with Figure 7a). To this the end, the
28 reconstructed time series indicates the occurrence of two phytoplankton blooms every year.
29 The first and larger bloom occurs in late austral summer (March-April), and a second smaller
30 bloom occurs in October coinciding with the development of spring blooms in the adjacent
31 Tasman Sea (Tilburg *et al.*, 2002).

1 3.3 Event Analysis (2005-2014)

2 When using window-averaged data, a standard cross-correlation analysis between upwelling
3 index, OC3 or FLH data and river discharges does not give satisfactory results. Overall, the
4 resultant correlation coefficients are insignificantly small and strongly biased by data
5 smoothing and interpolation. Instead of this, statistically more relevant information can be
6 derived from an event-based analysis, whereby all relevant data are averaged onto 8-day data
7 segments. Each data segment is defined as an individual event. The underlying assumption is
8 that phytoplankton blooms follow within ~3-7 days that after a nutrient-supply event. This
9 implies that there is a relatively high probability that both the physical event and the
10 ecological response occur within the timescale (8 days) of a data segment. This assumption is
11 consistent with observational evidence (Wilkerson *et al.*, 2006).

12 This approach, for instance, returns histograms of (reconstructed) chlorophyll-a ranges for the
13 study region in comparison with the Bonney upwelling region (**Figure 11**). Higher levels >1.5
14 mg/m^3 can be interpreted as phytoplankton blooms. Such levels are found off the Bonney
15 coast ~18.4% of time, which is equivalent to roughly 67 days per year. In the study region,
16 high chlorophyll-a levels $>1.5 \text{ mg/m}^3$ occurred 14.6% of time, which corresponds to around
17 53 days per year. Stronger phytoplankton blooms of chlorophyll-a concentrations $>2.5 \text{ mg/m}^3$
18 occur 5.4% of time or 19.8 days per year off the Bonney coast and 2.4% of time or 8.6 days
19 per annum on the western Tasmanian shelf.

20 A quick analysis (not shown) of other relevant parameters reveals a slightly higher frequency
21 of upwelling-favourable (~60% of time) than downwelling-favourable wind conditions.
22 Despite its irregularity, the discharge of the Davey River is relatively weak ($<25 \text{ m}^3/\text{s}$) for
23 ~42% of time (150 days per annum), whereas strong discharges ($>75 \text{ m}^3/\text{s}$) occur ~17% of
24 time (60 days per annum). When averaged on 8-day data segments, most (~59% of time) wind
25 events attain wind stresses in a range of 0.1 to 0.2 Pa, whereas storm events of wind stresses
26 $>0.3 \text{ Pa}$ are relatively rare ($<6\%$ of time).

27 When grouping data segments into different intervals of upwelling index and river discharge,
28 the largest number of records exist for large values of the upwelling index $>0.25 \text{ m}^2/\text{s}$ in the
29 presence of relatively low river discharge $<25 \text{ m}^3/\text{s}$ (**Table 1**). This criterion returns 113 of the
30 total of 425 events, noting that 10.6% of the 113 events are invalid due to cloud bias (**Table**
31 **2**). On the other hand, a relatively large number of events exists for stronger river discharges
32 $>50 \text{ m}^3/\text{s}$ and negative values of the upwelling index, returning 81 events of which 43.2% are

1 invalid due to cloud bias. This criterion corresponds to periods of enhanced river discharges,
2 typically occurring during austral winter and spring months (see Figure 7c), which is also the
3 time when strong northerly wind events and when the cloud bias is worst (see Table 2). The
4 other intervals considered have statistically satisfactory population sizes between 9 and 29
5 valid events.

6 Consistent with the aforementioned weak cross-correlations between parameters, average
7 chlorophyll-a concentrations are of the same order of magnitude in each parameter interval
8 considered (**Figure 12a**). This implies, for instance, that stronger upwelling-favourable winds
9 do not always create phytoplankton blooms. The only exception is the clear reduction of
10 chlorophyll-a concentration in austral winter months (see Figure 7b), which coincides with
11 strong river discharges and downwelling-favourable winds.

12 With a focus on events of phytoplankton blooms of chlorophyll-a concentrations $>1.5\text{mg/m}^3$
13 the outcome is vastly different (**Figure 12b**). Here, the by far largest number of blooms
14 occurs for stronger upwelling favourable winds ($\text{UI} > 0.25 \text{ m}^2/\text{s}$) yielding a total of 48.4% of
15 64 events. 50% of these events occur during low river discharges, which is characteristic of
16 the austral summer season. Hence, these events can be attributed to the classical wind-driven
17 upwelling mechanism.

18 Note that the proportion of such phytoplankton blooms increases from 48.4% to 69% when
19 accounting for upwelling favourable wind events with $\text{UI} > 0.25 \text{ m}^2/\text{s}$ in preceding data
20 segments. Hence, more than two thirds of the phytoplankton blooms on the west Tasmanian
21 shelf can be attributed to coastal winds. The remainder events are mainly associated with
22 October spring blooms, which are regular features of the study region (see Figure 10b).

23 While the outcome from the viewpoint of phytoplankton blooms gives conclusive results,
24 there are a total of 145 events with $\text{UI} > 0.25 \text{ m}^2/\text{s}$ during the study period of which only 39
25 (22%) triggered a phytoplankton bloom with chlorophyll-a concentrations exceeding 1.5
26 mg/m^3 . Another 13 events follow when accounting for UI values of the preceding data
27 segment, which brings the total to 30.0%. A number of possible processes could explain these
28 missing phytoplankton blooms including a) inference with river plumes that operate to
29 suppress phytoplankton blooms, b) lack of sufficiently long periods of relaxed wind after
30 upwelling events (Wilkerson *et al.*, 2006), c) preceding downwelling periods that create a
31 southward geostrophic coastal current and offshore transport in the bottom Ekman layer that,
32 due to inertia effects, resist subsequent wind changes, d) incursions of nutrient-low water

1 from the South Australian Current, and e) nutrient limitation. A more detailed analysis of
2 possible causes of the missing blooms is beyond the scope of this study.

3 In order to compare phytoplankton productivity between the Bonney upwelling system and
4 the west Tasmanian shelf, we assume that a) the spatial extent of their productivity zones is
5 similar, and b) eight-day composite values of reconstructed chlorophyll-a concentration are
6 proportional to the amount of phytoplankton formed during the eight-day period. To this end
7 we define a “relative productivity” as the time integral of eight-day composite chlorophyll-a
8 values. This assumption gives a total 289 mg (per unit volume) in relative production for the
9 west Tasmanian shelf (Table 3), which is about 81.4% that of the Bonney upwelling region.
10 With a focus on phytoplankton blooms with chlorophyll-a concentrations $>1.5 \text{ mg/m}^3$, the
11 west Tasmanian shelf still accounts for 70% of the relative production of the Bonney
12 upwelling region. When exclusively considering rarer events of high chlorophyll-a
13 concentrations $>2.5 \text{ mg/m}^2$, the relative productivity of the west Tasmanian shelf reduces to
14 40% with reference to the Bonney upwelling region.

15

16 **4 Conclusions**

17 A detailed analysis of satellite-derived ocean colour data for the periods 1998-2000 and 2005-
18 2014 suggest that the west Tasmanian shelf accommodates a highly productive ecosystem.
19 This region forms another significant upwelling centre of the Great South Australian Coastal
20 Upwelling System. The addition of this newly discovered upwelling centre, that the author
21 refers to as “West Tasmanian Upwelling”, makes this upwelling system one of the largest
22 (total spatial extension $\sim 1500 \text{ km}$) seasonal coastal upwelling systems on Earth.

23 The accuracy of satellite radar altimeter sea surface height measurement degrades in coastal
24 region (Roesler *et al.*, 2013) and cannot be used to identify upwelling jets on the western
25 Tasmanian shelf. Nevertheless, classical upwelling theory suggests the existence of such jets
26 on the west Tasmanian shelf. The significance of these upwelling jets is that they operate to
27 disperse nutrient-rich water northward along the shelf and possible into western Bass Strait.
28 This advective process would explain elevated chlorophyll-a levels in western Bass Strait – a
29 typical feature of the region during austral summer months (see Figure 3a). As such,
30 upwelling on the west Tasmanian shelf presumably constitutes an important nutrient source
31 for western Bass Strait waters.

1 **Acknowledgements**

2 The author thanks Paul Sandery (Bureau of Meteorology, Australia) for the provision of Cape
3 Grim wind data and Emlyn Jones (CSIRO, Australia), who pointed out the unreliability of
4 NASA-OC3 data for the west Tasmanian shelf. This work has not received external funding.

5 The author declares that there is no conflict of interests regarding the publication of this
6 paper.

7

1 **References**

- 2 Chen, C., Zhu, J., Beardsley, R. C., and Franks, P. J. S.: Physical-biological sources for dense
3 algal blooms near the Changjiang River, *Geophys. Res. Lett.*, 30(10), 1515,
4 doi:10.1029/2002GL016391, 2003.
- 5 Conolly, J. R. and Von der Borch, C. C.: Sedimentation and physiography of the sea floor
6 south of Australia, *Sediment. Geol.*, 1, 181-220, doi: 10.1016/0037-0738(67)90059-0, 1967.
- 7 Cresswell, G.: Currents of the continental shelf and upper slope of Tasmania. *Papers and*
8 *Proceedings of the Royal Society of Tasmania*, 133 (3), 21-30, 2000.
- 9 Gibbs, C. F., Tomczak, M., and Longmore, A. R.: The nutrient regime of Bass Strait,
10 *Australian J. Marine Freshwater Res.*, 37, 451-466, 1986.
- 11 Griffin, D. A., Thompson, P. A., Bax, N. J., and Hallegraeff, G. M.: The 1995 mass mortality
12 of pilchards: no role found for physical or biological oceanographic factors in Australia,
13 *Australian J. Marine Freshwater Res.*, 48, 27-58, 1997.
- 14 Hamer, D. J. and Goldsworthy, S. D.: Seal-fishery interactions: identifying the environmental
15 and operational aspects of a trawl fishery that contribute to by-catch and mortality of
16 Australian fur seals (*Arctocephalus pusillus doriferus*). *Biol. Conserv.*, 130, 517-529, 2006.
- 17 Herzfeld, M.: The annual cycle of sea surface temperature in the Great Australian Bight,
18 *Progress Oceanogr.*, 39(1), 1-27, doi: 10.1016/S0079-6611(97)00010-4, 1997.
- 19 Kämpf, J., Doubell, M., Griffin, D., Matthews, R. L., and Ward, T. M.: Evidence of a large
20 seasonal coastal upwelling system along the southern shelf of Australia, *Geophys. Res. Lett.*,
21 31, L09310, doi:10.1029/2003GLO19221, 2004.
- 22 Kämpf, J.: On the preconditioning of coastal upwelling in the eastern Great Australian Bight,
23 *J. Geophys. Res. Oceans*, 115, C12071, 11 pp., doi:10.1029/2010JC006294, 2010.
- 24 Lewis, R. K.: Seasonal upwelling along the southeastern coastline of South Australia,
25 *Australian J. Marine Freshwater Res.*, 32, 843-854, 1981.
- 26 Mann, K. H. and J. R. N. Lazier: *Dynamics of Marine Ecosystems: Biological-Physical*
27 *Interactions in the Oceans*, Oxford, Blackwell Publishing Ltd, 2006.

1 Middleton, J. F., Arthur, C., van Ruth, P., Ward, T., McClean, J., Maltrud, M., Gill, P., and
2 Middleton, S.: ENSO effects and upwelling along Australia's southern shelves, *J. Phys.*
3 *Oceanogr.*, 37(10), 2458-2477, 2007.

4 Rao, C. P. and Green, D. C.: Oxygen- and carbon-isotope composition of cold shallow-marine
5 carbonates of Tasmania, Australia, *Marine Geol.*, 53, 117-129, doi:10.1016/0025-
6 3227(83)90037-3, 1983.

7 Rao, C. P. and Adabi, M. H.: Carbonate minerals, major and minor elements and oxygen and
8 carbon isotopes and their variation with water depth in cool, temperate carbonates, western
9 Tasmania, Australia. *Marine Geol.*, 103, 249-272, doi: 10.1016/0025-3227(92)90019-E, 1992.

10 Ridgway, K. R. and Condie, S. A.: The 5500-km-long boundary flow off western and
11 southern Australia, *J. Geophys. Res.-Oceans* 109(4), c04017, doi:10.1029/2003JC001921,
12 2004.

13 Rochford, D. J.: A review of possible upwelling situation off Port MacDonal, South
14 Australia, CSIRO Australian Division Oceanography Report No. 81, 4 pp., 1977.

15 Roesler, C. J., Emery, W. J., and Kim, S. Y.: Evaluating the use of high-frequency radar
16 coastal currents to correct satellite altimetry. *J. Geophys. Res. Oceans*, 118 (7), 3240–3259,
17 doi: 10.1002/jgrc.20220, 2013.

18 Sandery, P. A. and Kämpf, J.: Winter-Spring Flushing of Bass Strait, South-Eastern Australia:
19 A numerical modelling study, *Est. Coast. Shelf Sci.*, 63, 23-31, doi:
20 10.1016/j.ecss.2004.10.009, 2005.

21 Sandery, P. A. and Kämpf, J.: Transport timescales for identifying seasonal variation in Bass
22 Strait, south-eastern Australia, *Est. Coast. Shelf Sci.* 74(4), 684-696,
23 doi:10.1016/j.ecss.2007.05.011, 2007.

24 Schahinger, R. B.: Structure of coastal upwelling events observed off the southern coast of
25 South Australia during Feb 1983-April 1984, *Australian J. Marine Freshwater Res.*, 38, 439-
26 459, 1987.

27 Shanmugam, P.: A new bio-optical algorithm for the remote sensing of algal blooms in
28 complex ocean waters, *J. Geophys. Res.*, 116, C04016, doi:10.1029/2010JC006796, 2011.

29 Tilburg, C. E., Subrahmanyam, B., and O'Brien, J. J.: Ocean color variability in the Tasman
30 Sea. *Geophys. Research Lett.*, 29(10), doi:10.1029/2001GL014071, 2002.

- 1 Tomczak, M.: The Bass Strait water cascade during winter 1981, *Cont. Shelf Res.*, 2, 55-87,
2 1985.
- 3 Ward, T. M., McLeay, L. J., Dimmlich, W., Rogers, A., McClatchie, S., Matthews, R. L.,
4 Kämpf, J., and Van Ruth, P. D.: Pelagic ecology of a northern boundary current system:
5 effects of upwelling on the production and distribution of sardine (*Sardinops sagax*), anchovy
6 (*Engraulis australis*) and southern bluefin tuna (*Thunnus maccoyii*) in the Great Australian
7 Bight. *Fishery Oceanogr.*, 15 (3), 191-207, doi: 10.1111/j.1365-2419.2006.00353.x, 2006.
- 8 Wass, R. E., Connolly, R. J., and MacIntyre, R. J.: Bryozoan carbonates and sand continuous
9 along southern Australia. *Marine Geol.* 9(1), 63-73, doi: 10.1016/0025-3227(70)90080-0,
10 1970. .
- 11 Wilkerson, F. P., Lassiter, A. M., Dugdale, R. C., Marchi, A., and Hogue, V. E.: The
12 phytoplankton bloom response to wind events and upwelled nutrients during the CoOP WEST
13 study, *Deep Sea Res. Part II*, 53, 3023–3048, 2006.
- 14 Xing, X.-G., Zhao, D.-Z., Liu, Y.-G., Yang, J.-H., Xiu, P., and Wang, L.: An overview of
15 remote sensing of chlorophyll fluorescence, *Ocean Sci. J.*, 42(1), 49-59, doi:
16 10.1007/BF030209102007, 2007.
- 17
18

1 Table 1. Number of Events of the Time Series (1/1/2005 to 31/3/2014) Grouped According to
 2 Different Intervals of Upwelling Index (UI) and River Discharge (R).

↓ R (m ³ /s)	UI (m ² /s) →	<-1/4	-1/4 to 0	0 to +1/4	>+1/4	all UI
<25		12	23	29	113	177
25 to 50		20	18	28	43	109
>50		81	14	20	24	139
all R		113	55	77	180	Σ = 425

3

4 Table 2. Percentage of Invalid Events due to Cloud Bias with Reference to Table 1.

↓ R (m ³ /s)	UI (m ² /s) →	<-1/4	-1/4 to 0	0 to +1/4	>+1/4	all UI
<25		25.0%	21.7%	27.6%	10.6%	15.8%
25 to 50		20.0%	27.8%	21.4%	32.6%	26.6%
>50		43.2%	21.4%	25.0%	37.5%	37.4%
all R		37.2%	23.6%	24.7%	19.7%	

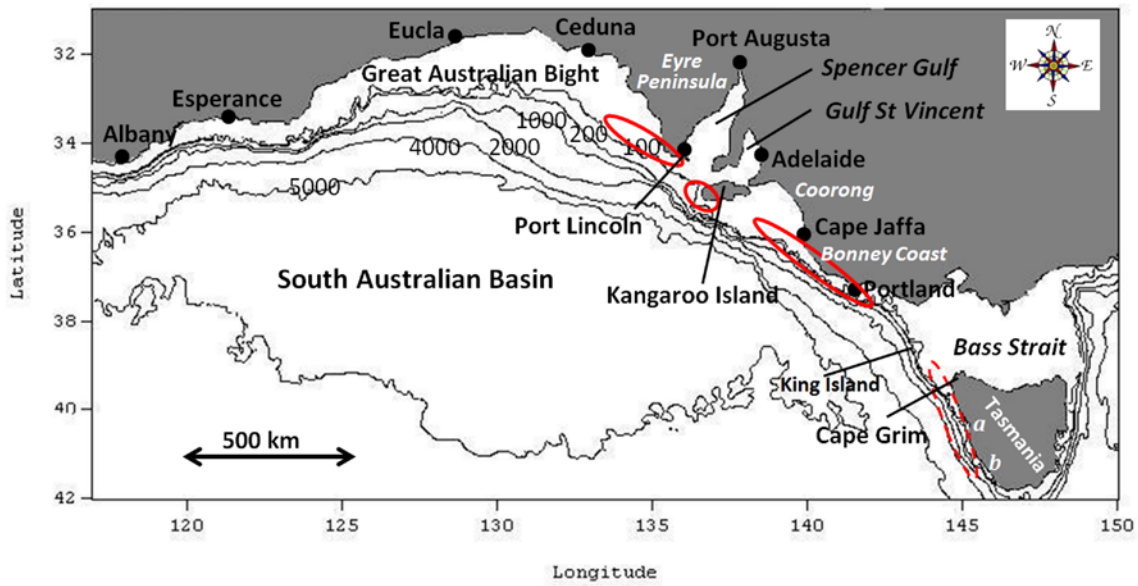
5

6 Table 3. Relative Production (mg/m³) for the Bonney Coast and the West Tasmanian Shelf
 7 (1/1/2005 to 31/3/2014) for Different Chlorophyll-a Thresholds.

Criterion	Bonney Coast	West Tasmanian Shelf	% of Bonney coast
All events	355.4	289.3	81.4%
Events with chl-a >1.5 g/m ³	180.0	126.4	70.2%
Events with chl-a >2.0 g/m ³	108.0	48.8	45.2%
Events with chl-a >2.5 g/m ³	79.1	31.1	39.3%

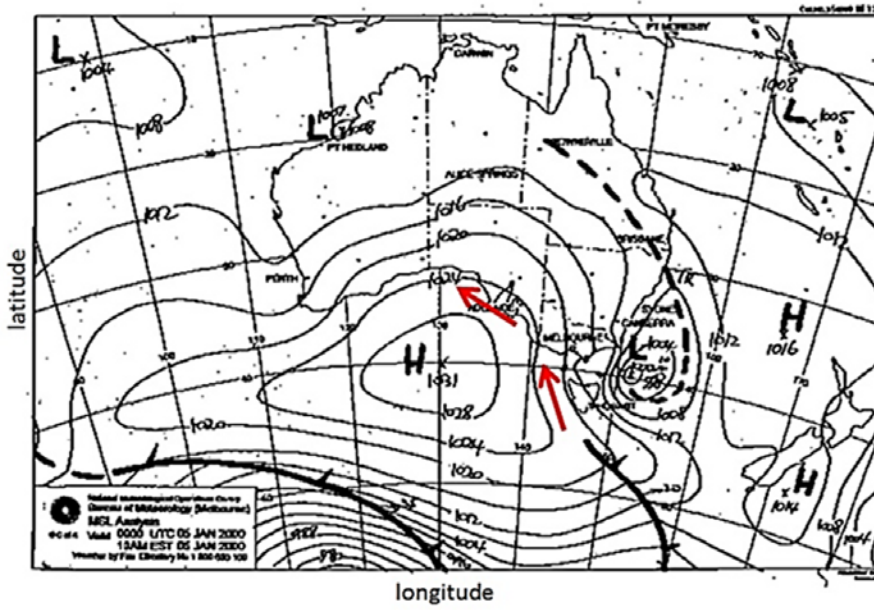
8

9



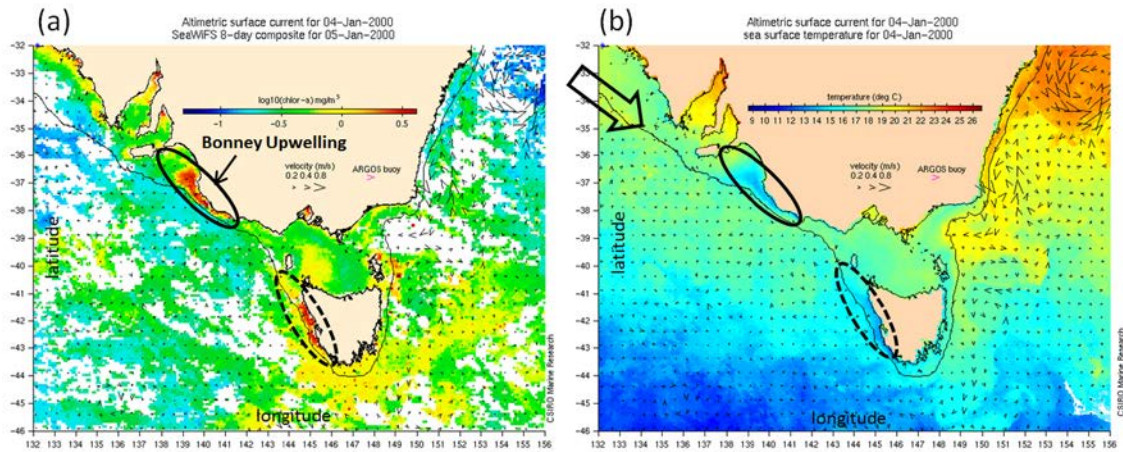
1
2
3
4
5
6
7

Figure 1. The geography of Australia's southern shelves. Isobath depths are in meters. Solid-line ellipses display known locations of coastal upwelling centers. The dashed-line ellipse highlights the region investigated in this paper. Letters a and b indicate the locations of the mouths of the Macquarie Harbour estuary and the Davey River.



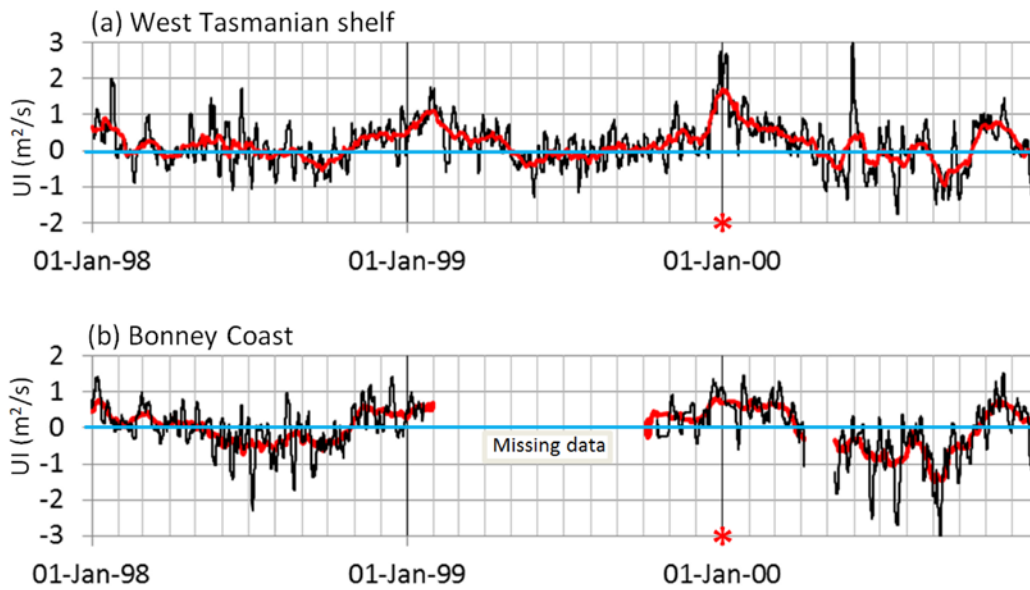
1
2
3
4
5
6

Figure 2. Mean sea level pressure for 6th January 2000, courtesy of the Bureau of Meteorology (Australia). Arrows indicate upwelling-favourable coastal winds, influenced by a blocking, low-pressure cell over Tasmania.



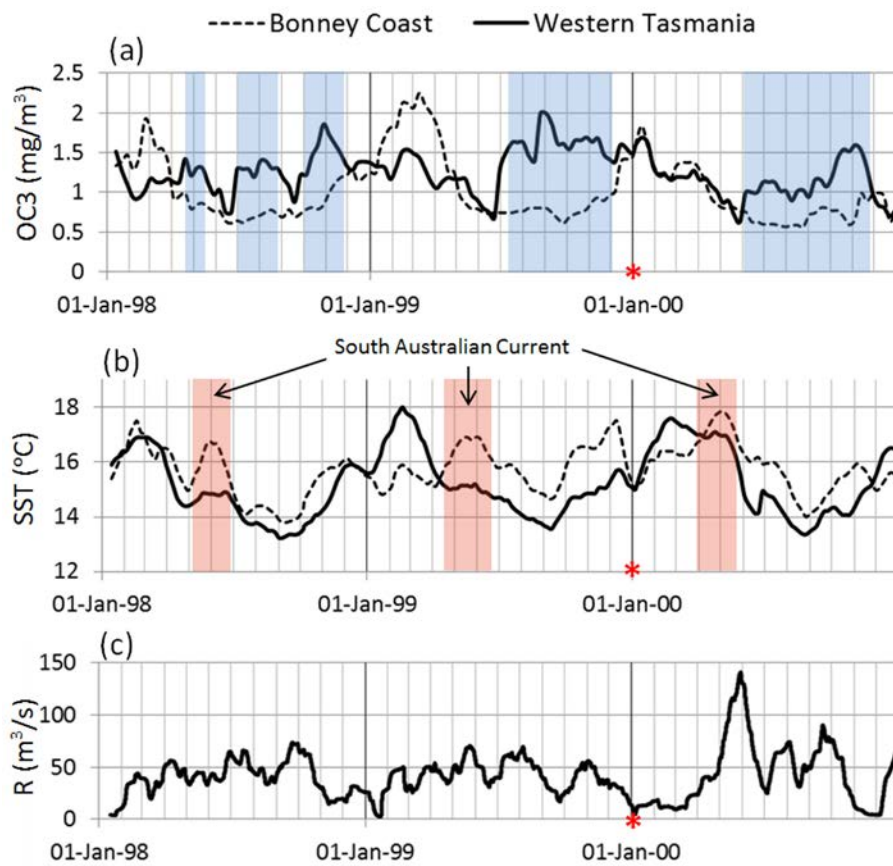
1
2
3
4
5
6
7
8

Figure 3. Occurrence of a pronounced coastal upwelling event in early January 2000, evident in satellite-derived distributions of a) MODIS-OC3 chlorophyll-a and b) sea surface temperature. White regions in panel a) are missing data due to clouds. The large arrow in panel b) indicates the pathway of the South Australian Current. Data source: South East Fishery ocean movies, David Griffin, CSIRO, <http://www.marine.csiro.au/~griffin/SEF/>.



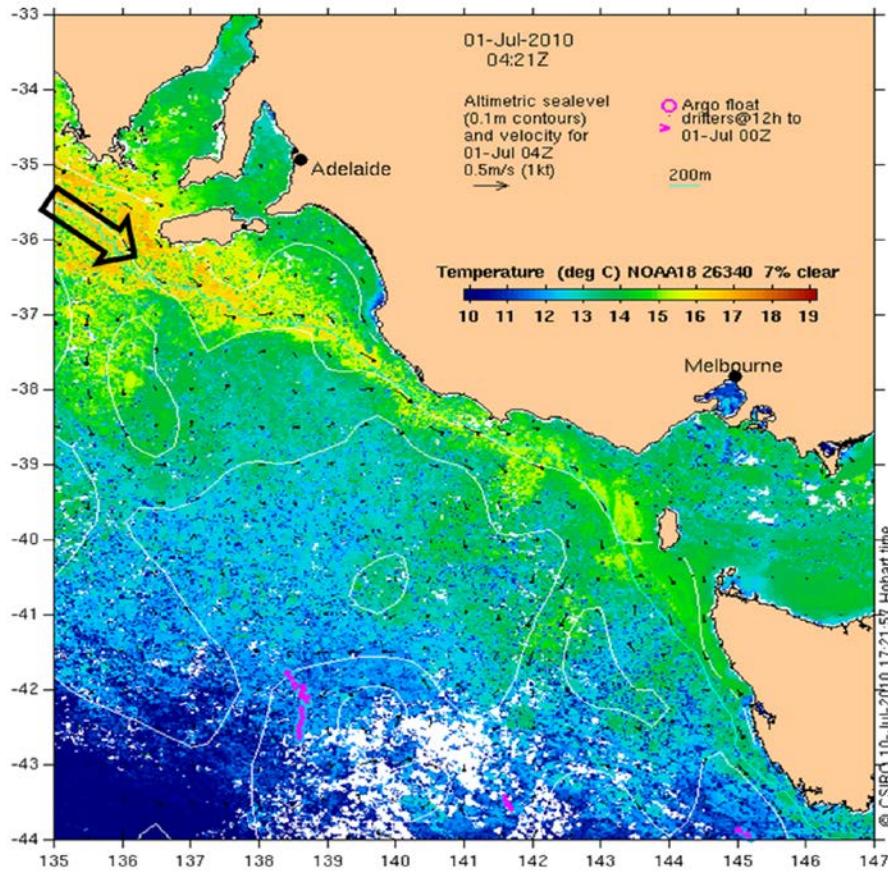
1
2
3
4
5
6
7

Figure 4. Time series (1/1/98-31/12/00) of the upwelling index (m^2/s) for a) the west Tasmanian shelf and b) the Bonney Coast. Thin, black (thick, red) curves are 4-day (20-day) moving averages. Stars highlight an upwelling event in early January 2000, corresponding to the spatial distributions shown in Figure 3. Data source: Bureau of Meteorology, Australia.



1
 2 Figure 5. Time series (1/1/98-31/12/00) of satellite-derived data of a) OC3 (mg/m^3) and b) sea
 3 surface temperature (SST, $^{\circ}\text{C}$) for the Bonney coast and the west Tasmanian shelf, and c)
 4 discharge from the Davey River (m^3/s). Running averages over an interval of 24 days have
 5 been used for both OC3 and river discharge. A running average over 20 days has been applied
 6 to the SST data. Shaded areas of panel a) highlight periods of substantial differences between
 7 the time series. Shaded areas in panel b) denote intermittent warming created by the South
 8 Australian Current. Stars highlight an upwelling event in early January 2000, corresponding
 9 to the spatial distributions shown in in Figure 3. Data source: SEF ocean movies, David
 10 Griffin, CSIRO, Australia.

11
 12

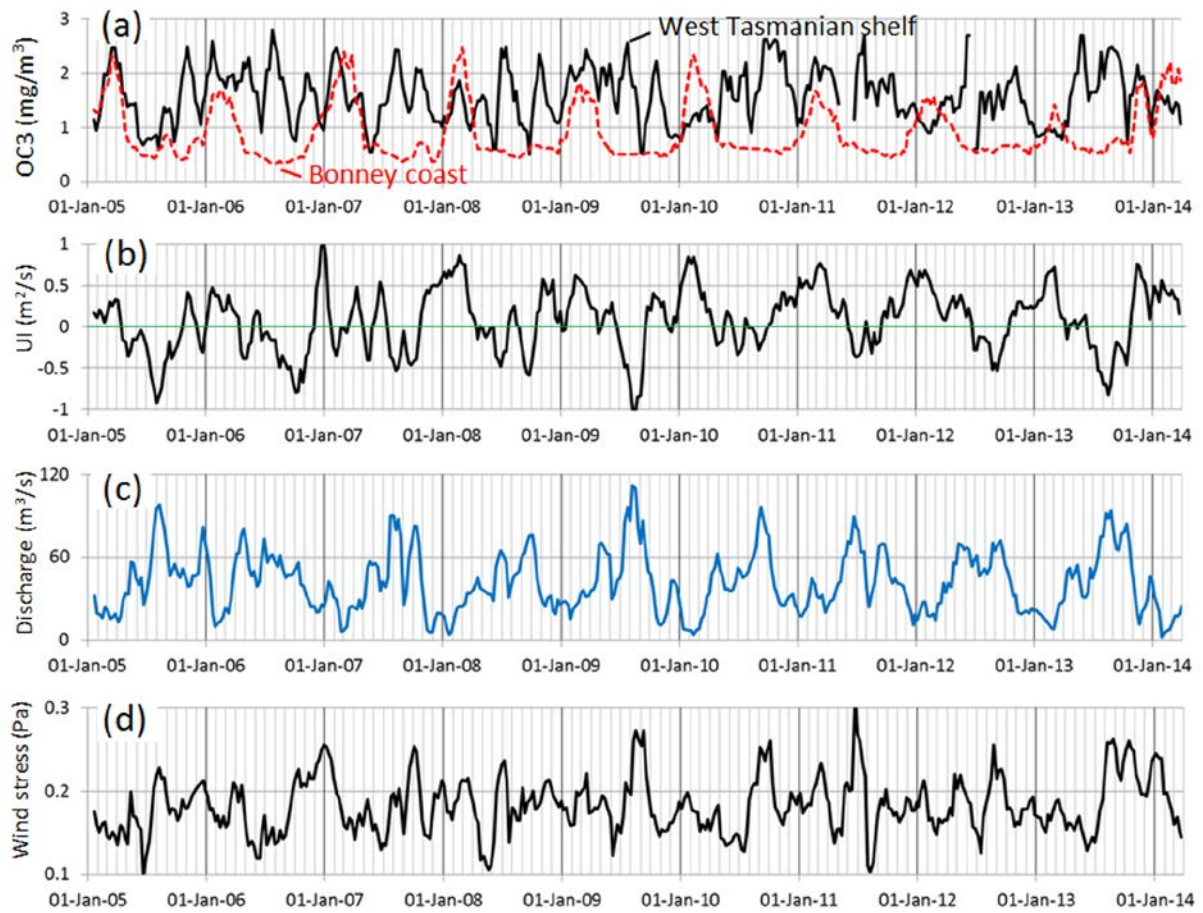


1

2

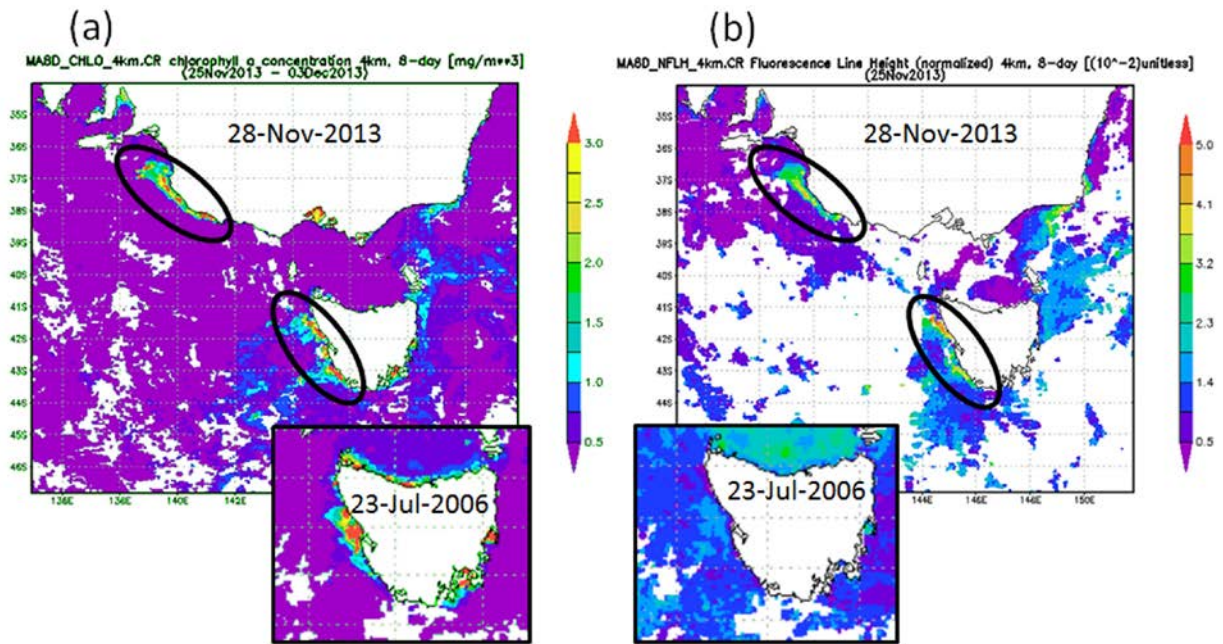
3 Figure 6. An example of the inflow of warm, nutrient-low South Australian Current that
 4 regularly appears along the Bonney coast and on the western Tasmanian shelf between May
 5 and July in every year. Data source: Integrated Marine Observing System (IMOS),
 6 <http://oceancurrent.imos.org.au/Adelaide/2010/2010070104.html>.

7



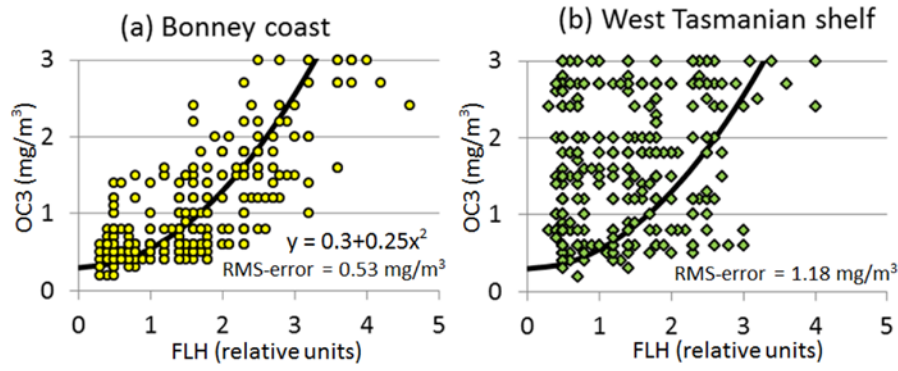
1
 2 Figure 7. Time series (1/1/2005-31/3/2014) of a) OC3, b) upwelling index, c) discharge from
 3 the Davey River, and d) wind stress. Data were first converted to 8-day segments and then
 4 smoothed with a running average over three segments. For comparison, panel a) includes data
 5 for the Bonney coast. Data sources: NASA (Giovanni), Bureau of Meteorology (Australia),
 6 and Water Information System of Tasmania.

7
 8



1
2
3
4
5
6

Figure 8. Snapshots of a) OC3 (mg/m^3) and b) normalised fluorescence line height (relative units) during a major upwelling event in late November 2013. The inserts show an example of a river discharge event in late July 2006. Data source: NASA (Giovanni).



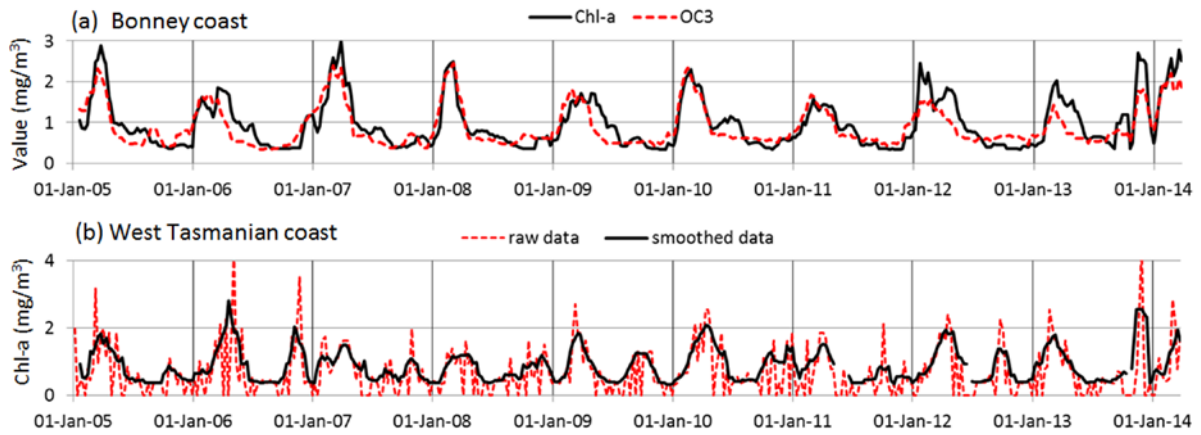
1

2 Figure 9. Correlation between OC3 values and normalized fluorescence line height (FLH),
 3 multiplied by a factor of 100, for a) the Bonney coast and b) the west Tasmanian shelf for the
 4 period 1/1/2005 to 31/3/2014. Solid lines show a quadratic regression corresponding to a
 5 Root-Mean-Square (RMS) error of 0.53 mg/m^3 for the Bonney coast data. Data source:
 6 NASA (Giovanni).

7

1

2

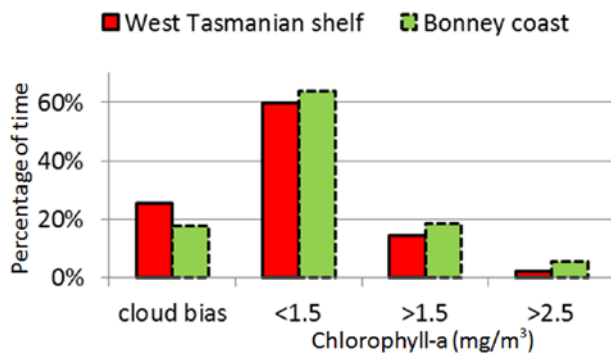


3

4 Figure 10. Reconstructed time series of chlorophyll-a concentrations (solid lines) from
5 normalized fluorescence line height (FLH) according to equation (2) for a) the Bonney coast
6 and b) the west Tasmanian shelf for the period 1-Jan-2005 to 31-March-2014. Shown are
7 running mean averages over three successive data segments. The dashed line in panel a)
8 shows the corresponding OC3 data. The dashed line in panel b) shows the raw 8-day
9 composite data with. Zero values (ignored in the averaging procedure) are allocated to
10 missing data due to cloud bias. Data source: NASA (Giovanni).

11

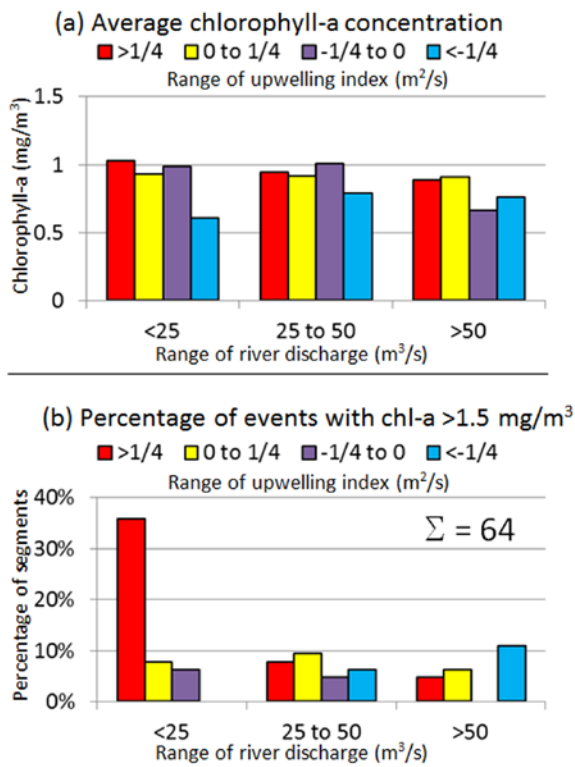
12



1

2 Figure 11. Event analysis. Histogram of 8-day segments for the period from 1/1/2005 to
 3 31/3/2014 that fall within certain ranges of chlorophyll-a concentrations for the west
 4 Tasmanian shelf and the Bonney coast. The result is expressed as time percentage with
 5 reference to the entire time period. “Cloud bias” refers to missing data.

6



1

2

3 Figure 12. Event analysis of the time series (1/1/2005 to 31/3/2014). a) Average chlorophyll-a
 4 values based on data segments that fall into certain intervals of upwelling index and discharge
 5 from the Davey River. The total number of segments is 316. b) Number of data segments of
 6 chlorophyll-a concentration >1.5 mg/m³, grouped as in panel a). 64 of the 316 data segments
 7 satisfy this condition.